Cyclotron resonance of interface magnetopolarons at finite temperatures

1998 J. Phys.: Condens. Matter 10 4857

(http://iopscience.iop.org/0953-8984/10/22/010)

J. Phys.: Condens. Matter **10** (1998) 4857–4866. Printed in the UK PII: S0953-8984(98)87278-0

Cyclotron resonance of interface magnetopolarons at finite temperatures

Bao-Hua Wei† and Chang Sub Kim

Department of Physics, Chonnam National University, Kwangju 500-757, Korea

Received 2 September 1997, in final form 13 March 1998

Abstract. Taking into account the interaction of an electron with interface optical phonons as well as bulk longitudinal optical phonons, we study the cyclotron resonance of magnetopolarons at the interfaces of polar crystals. We consider both the absorption and emission processes in our calculation using the Green's function method at finite temperatures. Consequently, different temperature characteristics of the cyclotron resonance mass and resonance frequency are found on either side of the off-resonance magnetic field region.

1. Introduction

Over the past few decades, there has been considerable research interest in the problem of surface and interface polarons in polar crystals, especially as regards the influence of magnetic fields and temperatures on the physical properties of the polaron [1–18]. The temperature dependence of the polaron mass in the absence of magnetic fields has been investigated theoretically by many authors, but the existing theories are still controversial. The various assumptions made regarding the mechanism of the electron–phonon interaction and the different theoretical methods applied have led to significantly different predictions for the behaviour of the polaron mass with temperature. In the early studies, using the Hartree method, Yokota calculated the energies of a polaron approximately and came to the conclusion that the polaron mass decreases with increasing temperature [7]; this picture was subsequently also obtained in references [8–10]. However, by using Gurari's variational method, Fulton obtained the opposite result [11]: the polaron mass was found to be an increasing function of temperature at finite temperatures; this was also the finding in references [1], [6], and [12]. A compromise between these opposite temperature dependences of the polaron mass was obtained by extending Feynman's polaron theory [13] to finite temperatures [14]. With this theory it was found that with increasing temperature the polaron mass first increases at low temperature, subsequently reaches a maximum value at a certain temperature, and at still higher temperature starts to decrease [14, 15]. However, for the presence of magnetic fields the theoretical efforts aimed at investigating the cyclotron resonances of the magnetopolaron have been carried out only for zero temperature [16–18]. Accordingly, it seems to be a worthwhile endeavour to study both the temperature and the magnetic field dependence of magnetopolarons in detail, using a more powerful theoretical method.

† Permanent address: Department of Applied Physics, South China University of Technology, Guangzhou, People's Republic of China.

0953-8984/98/224857+10$19.50

Electron–optical phonon interaction in polar crystals plays an important role in determining the physical characteristics of polarons. It is generally accepted that in bulk crystals the effective mass of an electron is enhanced by the virtual coupling of a quasi-free electron with bulk longitudinal optical (BO) phonons. However, even in investigations of the heterostructures, only electron–BO phonon interaction was considered and electron–interface optical (IO) phonon interaction was neglected (see for instance references [2, 15], and [17]). Recently, it was reported that, in obtaining the potential induced by the electron–phonon interaction, IO phonons must be considered together with BO phonons in quasi-two-dimensional (Q2D) systems, especially when the distance between the electron and the interface (or surface) is comparable to the radius of the polaron [19–21].

In this work, taking into account the interaction of an electron with both BO and IO phonons, we investigate theoretically the cyclotron resonance of polarons at the interfaces of polar crystals by using the powerful Green's function method for finite temperatures. Considering both the absorption resonance and the emission resonance, the dependence of the cyclotron resonance mass and of the cyclotron resonance frequency of the interface polaron on magnetic fields and temperatures around, but excluding, the resonant magnetic field region is studied. The resonant region was treated previously using the Rayleigh–Schrödinger perturbation method [5]. The calculated magnetic field dependence of the cyclotron resonance at zero temperature is consistent with the result obtained by a memory function approach [18]. In addition, we have obtained some new temperature characteristics of the resonance mass and resonance frequency in the presence of magnetic fields: the resonance mass (resonance frequency) increases (decreases) with temperature below the resonant field but decreases (increases) with temperature above the resonant field.

The reminder of the paper is organized as follows. In section 2 we introduce the effective Hamiltonian of the system considered, and section 3 provides a formulation for calculating the cyclotron resonance mass and cyclotron resonance frequency of the interface magnetopolaron. Our numerical results and a discussion are given in section 4. Finally, we will provide a brief conclusion in section 5.

2. The effective Hamiltonian

We consider a heterostructure composed of two semi-infinite polar crystals: polar crystal 1 in the $z > 0$ half-space and polar crystal 2 in the $z < 0$ half-space, whose interface is the xy-plane. For simplicity, the electron motion is restricted to the half-space $z > 0$, by assuming that there is an infinitely high barrier created by crystal 2. The static uniform magnetic field $\boldsymbol{B} = (0, 0, B)$ is applied along the z-direction and is described by a vector potential in the Landau gauge $\boldsymbol{A} = B(0, x, 0)$. In this work, we take into account the interaction of an electron with both BO phonons in the $z > 0$ half-space and IO phonons. Also, we include an image potential produced by the polarization induced on the interface due to the electron. Under the isotropic effective-mass approximation, the Hamiltonian of our electron–phonon system can be written as follows [19]:

$$H = H_{\parallel} + H_{\perp} \qquad H_{\parallel} = H_0 + H_I \qquad H_I = H_{e-BO} + H_{e-IO} \tag{1}$$

where

$$H_0 = \frac{p_x^2}{2m_b} + \frac{1}{2m_b}\left(p_y + \frac{\beta^2}{2}x\right)^2 + \sum_{\boldsymbol{k}} \hbar\omega_{BO} a_{\boldsymbol{k}}^{+} a_{\boldsymbol{k}} + \sum_{\boldsymbol{q}} \hbar\omega_{IO} b_{\boldsymbol{q}}^{+} b_{\boldsymbol{q}} \tag{2}$$

$$H_{\perp} = \frac{p_z^2}{2m_b} + \frac{e^2(\epsilon_{\infty 1} - \epsilon_{\infty 2})}{4z\epsilon_{\infty 1}(\epsilon_{\infty 1} + \epsilon_{\infty 2})} \tag{3}$$

and

$$H_{e-BO} = \sum_{\boldsymbol{k}} \left(V_{\boldsymbol{k}}^* \sin(zk_z) \exp(-\mathrm{i}\boldsymbol{k}_\parallel \cdot \boldsymbol{\rho}) a_{\boldsymbol{k}}^+ + \mathrm{HC} \right) \tag{4}$$

$$H_{e-IO} = \sum_{\boldsymbol{q}} \left(C_{\boldsymbol{q}}^* \exp(-qz) \exp(-\mathrm{i}\boldsymbol{q} \cdot \boldsymbol{\rho}) b_{\boldsymbol{q}}^+ + \mathrm{HC} \right) \tag{5}$$

are the contributions from the electron interaction with BO phonons and with IO phonons, respectively. In the above equations, the following notation has been used:

$$V_{\boldsymbol{k}}^* = \frac{\mathrm{i}}{|\boldsymbol{k}|} \left(\frac{4\pi e^2}{\epsilon V} \hbar\omega_{BO} \right)^{1/2} \qquad C_{\boldsymbol{q}}^* = \mathrm{i} \left(\frac{\pi e^2}{q\epsilon^* S} \hbar\omega_{IO} \right)^{1/2} \tag{6}$$

$$\frac{1}{\epsilon} = \frac{1}{\epsilon_{\infty 1}} - \frac{1}{\epsilon_{01}} \qquad \frac{1}{\epsilon^*} = \frac{2}{\epsilon_{\infty 1} + \epsilon_{\infty 2}} - \frac{2}{\epsilon_{01} + \epsilon_{02}} \qquad \beta^2 = \frac{2eB}{c} \tag{7}$$

and $\boldsymbol{\rho} = (x, y, 0)$ is the projection of the electron position vector on the xy-plane. Also, $\boldsymbol{p} = (p_x, p_y, p_z)$ is the momentum of the electron, $\boldsymbol{k} = (\boldsymbol{k}_\parallel, k_z)$ is the wave vector of the BO phonons; $\boldsymbol{q}$ is the 2D wave vector of IO phonons, $a_{\boldsymbol{k}}^+$ ($a_{\boldsymbol{k}}$) and $b_{\boldsymbol{q}}^+$ ($b_{\boldsymbol{q}}$) are the creation (annihilation) operators of BO and IO phonons, respectively, and ω_{BO} and ω_{IO} are the frequencies of BO phonons and IO phonons, respectively. The first two terms in H_0 describe the kinetic energy of the 2D motion of the electron in the xy-plane, which forms Landau energy levels, and the third and fourth terms are the energies of BO and IO phonons, respectively. The first term in $H_\perp$ is the kinetic energy of the electron in the z-direction, and the second one is the image potential. The volume of crystal 1 is denoted by V, and the area of its interface is denoted by S. Also, $\epsilon_{\infty 1}$ ($\epsilon_{\infty 2}$) and ϵ_{01} (ϵ_{02}) are the optical and static dielectric constants of crystal 1 (crystal 2), respectively.

The relation between the frequency of bulk transverse optical phonons ω_{TO} and that of the BO phonons ω_{BO} is determined by the Lyddane–Sachs–Teller relation

$$\frac{\omega_{BO}^2}{\omega_{TO}^2} = \frac{\epsilon_{01}}{\epsilon_{\infty 1}} \tag{8}$$

and the frequencies of BO and IO phonons satisfy the equality

$$\omega_{BO}^2 = \omega_{TO}^2 \frac{\epsilon_{\infty 1}(\epsilon_{01} + \epsilon_{02})}{\epsilon_{01}(\epsilon_{\infty 1} + \epsilon_{\infty 2})}. \tag{9}$$

The coupling constants of the electron with BO phonons and the electron with IO phonons are given by

$$\alpha_B = \frac{e^2}{2\hbar} \left(\frac{2m_b}{\hbar\omega_{BO}} \right)^{1/2} \frac{1}{\epsilon} \qquad \alpha_I = \frac{e^2}{2\hbar} \left(\frac{2m_b}{\hbar\omega_{IO}} \right)^{1/2} \frac{1}{\epsilon^*}. \tag{10}$$

The cyclotron resonance frequency of an electron with the bare band effective mass m_b is

$$\omega_c = \frac{eB}{m_b c}. \tag{11}$$

For subsequent usage, we define

$$\lambda_B^2 = \frac{\omega_c}{\omega_{BO}} \qquad \lambda_I^2 = \frac{\omega_c}{\omega_{IO}}. \tag{12}$$

At finite temperatures, we choose $|n_{\boldsymbol{k}}, n_{\boldsymbol{q}}\rangle$ as the wavefunction for describing the phonon state, in which $n_{\boldsymbol{k}}$ and $n_{\boldsymbol{q}}$ represent the numbers of BO and IO phonons, respectively. When the temperature is lower than the room temperature, even though the phonon frequency will decrease with increasing temperature, we can still take them as constant because of the

small relative change of the frequency (≈1%) [22]. Also, the energies of the interactions between the electron and the phonons are much smaller than the phonon energy except in the strong-coupling case. Accordingly, we may assume that the eigenvalues of $a_{\boldsymbol{k}}^{+}a_{\boldsymbol{k}}$ and $b_{\boldsymbol{q}}^{+}b_{\boldsymbol{q}}$ in the phonon state are approximately equal to the equilibrium values [10], i.e.

$$\langle n_{\boldsymbol{k}}\rangle = \langle a_{\boldsymbol{k}}^{+}a_{\boldsymbol{k}}\rangle = \frac{1}{\exp(\overline{h}\omega_{BO}/k_BT)-1} \tag{13}$$

$$\langle n_{\boldsymbol{q}}\rangle = \langle b_{\boldsymbol{q}}^{+}b_{\boldsymbol{q}}\rangle = \frac{1}{\exp(\overline{h}\omega_{IO}/k_BT)-1} \tag{14}$$

where k_B is the Boltzmann constant.

The unperturbed energy corresponding to H_0 is given by

$$E_n^{(0)} = \varepsilon_n + \sum_{\boldsymbol{k}}\langle n_{\boldsymbol{k}}\rangle\overline{h}\omega_{BO} + \sum_{\boldsymbol{q}}\langle n_{\boldsymbol{q}}\rangle\overline{h}\omega_{IO} \tag{15}$$

where $\varepsilon_n = (n+\frac{1}{2})\overline{h}\omega_c$ is the electron Landau level with the Landau quantum number n. In the limit of weak electron–phonon coupling, H_I could be treated as a small perturbation. In this case, it suffices to calculate the contributions to the electron proper self-energy part by retaining the lowest-order skeleton diagram. Using the standard Green's function method [20], the total proper self-energy part of electron is given by

$$\Sigma^{*}(s,z,\mathrm{i}\omega_l) = \Sigma_{BO}^{*}(s,z,\mathrm{i}\omega_l) + \Sigma_{IO}^{*}(s,z,\mathrm{i}\omega_l) \tag{16}$$

where $\Sigma_{BO}^{*}(s,z,\mathrm{i}\omega_l)$ and $\Sigma_{IO}^{*}(s,z,\omega_l)$ are the electron self-energy parts corresponding to the H_{e-BO} and H_{e-IO}, respectively [19], which are given as

$$\begin{aligned}\Sigma_{BO}^{*}(s,z,\mathrm{i}\omega_l) &= -\frac{1}{\beta}\sum_{s',\boldsymbol{k},\nu_{l'}} G^{(0)}[s',\mathrm{i}(\omega_l-\nu_{l'})]|f_{s,s'}(z,\boldsymbol{k})|^2 D_{BO}^{(0)}(\boldsymbol{k},\mathrm{i}\nu_{l'}) \\ &= \frac{1}{\overline{h}}\sum_{s',\boldsymbol{k}}|f_{s,s'}(z,\boldsymbol{k})|^2\left[\frac{\langle n_{\boldsymbol{k}}\rangle + n_{s'}}{\mathrm{i}\omega_l-\omega_{s'}+\omega_{BO}} + \frac{\langle n_{\boldsymbol{k}}\rangle + 1 - n_{s'}}{\mathrm{i}\omega_l-\omega_{s'}-\omega_{BO}}\right]\end{aligned} \tag{17}$$

$$\begin{aligned}\Sigma_{IO}^{*}(s,z,\mathrm{i}\omega_l) &= -\frac{1}{\beta}\sum_{s',\boldsymbol{q},\nu_{l'}} G^{(0)}[s',\mathrm{i}(\omega_l-\nu_{l'})]|f_{s,s'}(z,\boldsymbol{q})|^2 D_{IO}^{(0)}(\boldsymbol{q},\mathrm{i}\nu_{l'}) \\ &= \frac{1}{\overline{h}}\sum_{s',\boldsymbol{q}}|f_{s,s'}(z,\boldsymbol{q})|^2\left[\frac{\langle n_{\boldsymbol{q}}\rangle + n_{s'}}{\mathrm{i}\omega_l-\omega_{s'}+\omega_{IO}} + \frac{\langle n_{\boldsymbol{q}}\rangle + 1 - n_{s'}}{\mathrm{i}\omega_l-\omega_{s'}-\omega_{IO}}\right].\end{aligned} \tag{18}$$

In the above equation, $f_{s,s'}(z,\boldsymbol{k})$ and $f_{s,s'}(z,\boldsymbol{q})$ are defined in reference [19], $G^{(0)}(s,\mathrm{i}\omega_l)$ and $D_{BO/IO}^{(0)}(\boldsymbol{k}/\boldsymbol{q},\mathrm{i}\nu_l)$ are the Matsubara Green's functions of free electrons and free phonons, respectively, where $\omega_l = (2l+1)\pi/\overline{h}\beta$ and $\nu_l = 2l\pi/\overline{h}\beta$ where l is an integer, and $\omega_s = (E_n-\mu)/\overline{h}$ where μ is the chemical potential, and $\langle n_s\rangle$ is the mean number of electrons. We continue $\mathrm{i}\omega_l$ analytically to the upper half of the complex ω-plane and take the form $\omega = (E_n^{*}-\mu)/\overline{h}$. From Dyson's equation, the retarded Green's function is obtained as [19]

$$G^{R}(s,z,E_n^{*}) = \frac{1}{E_n^{*}-E_n^{(0)}-\Sigma^{*}(s,z,E_n^{*})}. \tag{19}$$

The electron self-energy shift related to $H_{\|}$ is given approximately by

$$\Delta E_n(z) = \Sigma^{*}(s,z,E_n^{*}) = V_{e-BO}^{(n)}(z) + V_{e-IO}^{(n)}(z). \tag{20}$$

Then, we get the effective Hamiltonian in the form

$$H_{n,eff}(z) = E_n^{(0)} + \frac{p_z^2}{2m_b} + V_{eff}^{(n)}(z) \tag{21}$$

where the effective potential is written as

$$V_{eff}^{(n)}(z) = V_{im}(z) + \Delta E_n(z) \tag{22}$$

where $V_{im}(z)$ is the image-potential energy of the electron, which is given in the second term of equation (3).

For simplicity, we take into account only the lowest subband of $H_\perp$, so the relevant variational wavefunction with the variational parameter ξ_n can be selected as [20]

$$\phi_n(z) = 2\xi_n^{3/2}\exp(-\xi_n z) \tag{23}$$

and we finally come to its energy for the state with Landau quantum number n as follows:

$$\begin{aligned} E_n &= \langle\phi_n(z)|H_{n,eff}(z)|\phi_n(z)\rangle \\ &= \left(n+\frac{1}{2}\right)\overline{h}\omega_c + \sum_{\boldsymbol{k}}\langle n_{\boldsymbol{k}}\rangle\overline{h}\omega_{BO} + \sum_{\boldsymbol{q}}\langle n_{\boldsymbol{q}}\rangle\overline{h}\omega_{IO} + \frac{\overline{h}\xi_n^2}{2m_b} \\ &\quad + \frac{\xi_n e^2(\epsilon_{\infty 1}-\epsilon_{\infty 2})}{4\epsilon_{\infty 1}(\epsilon_{\infty 1}+\epsilon_{\infty 2})} + E_{e-BO}^{(n)}(\xi_n) + E_{e-IO}^{(n)}(\xi_n). \end{aligned} \tag{24}$$

The last two terms in equation (24) are the self-energies of the polaron contributed by the interaction of the electron with BO phonons and IO phonons, respectively, and the variational parameter ξ_n can be determined using

$$\frac{\partial E_n(\xi_n)}{\partial \xi_n} = 0. \tag{25}$$

The method of calculating the self-energy of the polaron is similar to that of our previous paper [20], and is not repeated here for the sake of conciseness.

3. Cyclotron frequency and cyclotron mass

In this work, we only consider the cyclotron resonance between the lowest subbands, which is of major interest in most experimental and theoretical studies. The cyclotron resonance frequency ω_c^* is defined to be

$$\omega_c^* = \frac{E_1(\xi_1) - E_0(\xi_0)}{\overline{h}}. \tag{26}$$

After a tedious but direct calculation, we obtain the self-energies of the interface magnetopolaron as

$$E_{e-BO(IO)}^{(0)}(\xi_0) = -\alpha_{B(I)}\lambda_{B(I)}\overline{h}\omega_{BO(IO)}\left\{\sum_{l=1}\frac{1}{l!}\left(\frac{\langle n_{\boldsymbol{k}(q)}\rangle+1}{l\lambda_{B(I)}^2+1} + \frac{\langle n_{\boldsymbol{k}(q)}\rangle}{l\lambda_{B(I)}^2-1}\right)I_{B(I)}(l,\xi_0)\right\} \tag{27}$$

$$\begin{aligned} E_{e-BO(IO)}^{(1)}(\xi_1) &= -\alpha_{B(I)}\lambda_{B(I)}\overline{h}\omega_{BO(IO)} \\ &\quad\times\left\{\sum_{l=1,l\neq 0}\frac{l+1}{l!}\left(\frac{\langle n_{\boldsymbol{k}(q)}\rangle+1}{l\lambda_{B(I)}^2+1} + \frac{\langle n_{\boldsymbol{k}(q)}\rangle}{l\lambda_{B(I)}^2-1}\right)I_{B(I)}(l,\xi_1)\right. \\ &\quad + \sum_{l=0,l\neq 1}\frac{1}{l!}\left(\frac{\langle n_{\boldsymbol{k}(q)}\rangle+1}{(l-1)\lambda_{B(I)}^2+1} + \frac{\langle n_{\boldsymbol{k}(q)}\rangle}{(l-1)\lambda_{B(I)}^2-1}\right)I_{B(I)}(l+1,\xi_1) \\ &\quad \left. - \sum_{l=1,l\neq 0}\frac{2}{l!}\left(\frac{\langle n_{\boldsymbol{k}(q)}\rangle+1}{l\lambda_{B(I)}^2+1} + \frac{\langle n_{\boldsymbol{k}(q)}\rangle}{l\lambda_{B(I)}^2-1}\right)I_{B(I)}(l+1,\xi_1)\right\} \end{aligned} \tag{28}$$

where

$$I_B(l,\xi_n) = \left(\frac{\sqrt{\hbar}\xi_n}{\beta}\right)^{2l+1} \int_0^\infty \mathrm{d}u \ \frac{u^3+3u^2+3u}{(1+u)^3} u^{2l} \exp\left(-\frac{\hbar\xi_n^2}{\beta^2}u^2\right) \tag{29}$$

$$I_I(l,\xi_n) = \left(\frac{\sqrt{\hbar}\xi_n}{\beta}\right)^{2l+1} \int_0^\infty \mathrm{d}u \ \frac{u^{2l}}{(1+u)^3} \exp\left(-\frac{\hbar\xi_n^2}{\beta^2}u^2\right). \tag{30}$$

In the above equation, we have taken into account both the absorption resonance and the emission resonance. The terms containing $\langle n\rangle + 1$ correspond to the emission of a virtual phonon during the electron–phonon interaction, and the terms containing $\langle n\rangle$ correspond to the absorption of a virtual phonon in the process of electron–phonon interaction. In the past, most studies have neglected the absorption resonance [11], but our numerical results show that both the processes must be considered at the same time at finite temperature, especially for the magnetopolaron.

Once the cyclotron resonance frequency, equation (26), is determined, the cyclotron resonance mass m^* of the interface magnetopolaron can be also obtained, using the relation [18]

$$\frac{m^*}{m_b} = \frac{\omega_c}{\omega_c^*}. \tag{31}$$

4. Numerical results and discussion

We choose a GaAs(crystal 1)/GaSb(crystal 2) heterostructure as a model for our numerical computation. The material parameters are taken from reference [1]: for GaAs, $\epsilon_{01} = 12.83$, $\epsilon_{\infty 1} = 10.90$, $\hbar\omega_{BO1} = 36.7$ meV, and $\alpha_{BO1} = 0.0675$; for GaSb, $\epsilon_{02} = 15.69$, $\epsilon_{\infty 2} = 14.44$, $\hbar\omega_{BO2} = 29.8$ meV, and $\alpha_{BO2} = 0.025$.

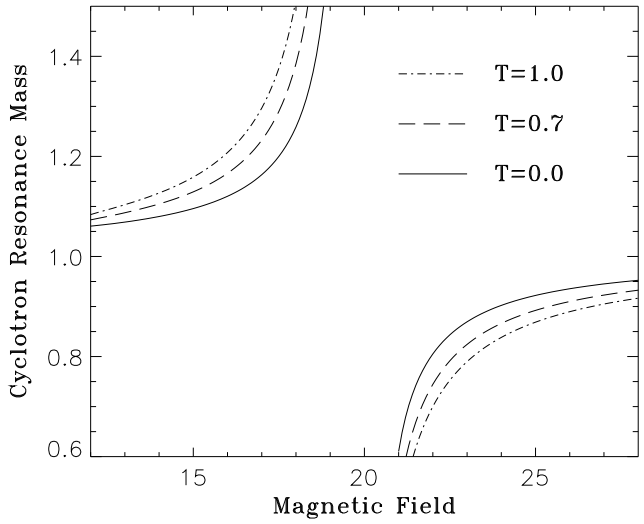

Figure 1. The cyclotron resonance mass m^* of the interface magnetopolaron as a function of the magnetic field for temperatures $T = 0.0, 0.7$, and $1.0\ T_D$ where $T_D = 426$ K; m^* and the magnetic field are in units of m_b and T, respectively.

In figure 1 the cyclotron resonance mass m^* of the interface magnetopolaron is depicted as a function of the magnetic field, in units of m_b, where the resonant magnetic field

region, $B_R \sim 20.8$ T, has been excluded. Several temperatures T have been considered; $T = 0, 0.7$, and 1.0, in units of the Debye temperature T_D, which is about 426 K for GaAs. Our numerical results show that for a given temperature the cyclotron resonance mass first slowly increases with the magnetic fields, and then increases sharply on approaching closer to the resonant region. After passing the resonant fields, the cyclotron resonance mass behaves oppositely to in the case below the resonance. It is also seen that each resonance mass saturates to a constant at very high magnetic fields. This tendency is consistent with the previous result of reference [18] obtained by a memory function approach at zero temperature. The resonant region was excluded in our numerical calculation since the Green's function method used fails to converge properly near the resonance. However, it has been studied in our previous paper utilizing another method [5]. Although we have not shown this, we have also observed that for a fixed temperature the cyclotron resonance frequency of the interface magnetopolaron decreases as the resonance field is approached from below B_R, while it decreases for magnetic fields above the resonance value.

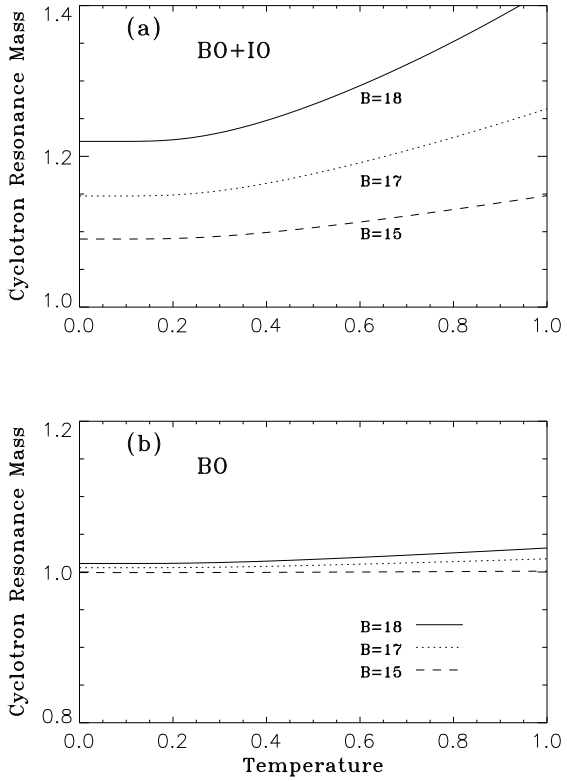

Figure 2. The temperature dependence of the cyclotron resonance mass m^* below the resonant field $B_R \sim 20.8$ T for several magnetic fields, $B = 15$, 17, and 18 T: (a) including both BO and IO phonon contributions; (b) including only the BO contribution. Here, m^* and the temperature are in units of m_b and $T_D = 426$ K, respectively.

Next, in order to see the temperature characteristics, we plot the cyclotron resonance mass m^* in figures 2(a) and 2(b) as a function of temperature for several magnetic fields $B = 15$, 17, and 18 T, below B_R. Figure 2(a) includes the effects of both BO and IO phonons. On the other hand, only the BO phonon contribution is included in

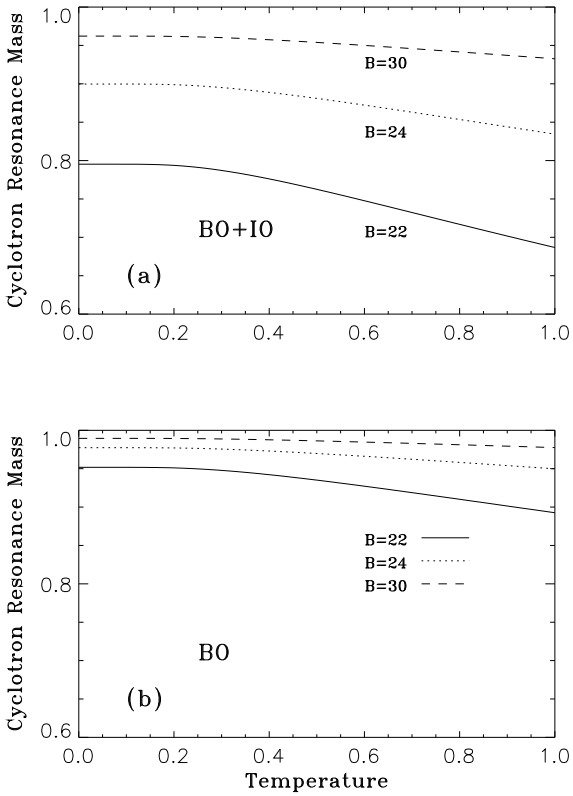

Figure 3. As figure 2, but for the fields $B = 22$, 24, and 30 T chosen above the resonant magnetic field B_R.

figure 2(b). And, the same figures are presented in figures 3(a) and 3(b) for above B_R, for $B = 22, 24,$ and 30 T. First of all, opposite temperature dependences of the cyclotron resonance mass below and above the resonant magnetic field region have been found. Below the resonance field, m^* increases with temperature. On the other hand, when $B > B_R$, m^* decreases with temperature. This temperature behaviour is consistent with our previous result obtained in investigating the potential induced by electron–phonon interaction [21]. By comparing figures 2(a) and 2(b) one can see that the contribution from IO phonons is not negligible, and furthermore the temperature characteristics are largely determined by the electron–IO phonon interaction. Also, the IO phonon effect is more sensitive to the magnetic fields. A similar feature is seen for the $B > B_R$ case in figures 3(a) and 3(b), but in this case the IO phonon effect is negative; that is, it reduces the values of m^* (see equations (27) and (28)). Although they are not illustrated, we have also seen different temperature characteristics for the resonance frequency: ω_c^* decreases with temperature when $B < B_R$ but it increases with temperature when $B > B_R$. The closer the magnetic field is to the resonant field, the steeper the change of the cyclotron resonance frequency is with temperature change. Also, at very high magnetic fields, the cyclotron resonance frequency of the magnetopolaron remains constant as the temperature changes, which corresponds to the saturation of the polar phonons.

As we mentioned in the introduction, there appears to be controversy in the literature as regards to the temperature characteristics of the polaron; the results vary depending on

the various electron–phonon interaction mechanisms assumed and the different theoretical methods used. In the present paper we have obtained interesting opposite temperature characteristics of the cyclotron resonance mass of magnetopolarons on either side of the off-resonance region by fully considering the electron–phonon interaction, using a powerful Green's function method. To our knowledge, few efforts have been made to investigate the temperature dependence of the cyclotron resonance of the polaron in the presence of magnetic fields. Neither have experiments been carried out to study simultaneously the temperature and magnetic field dependences of the cyclotron resonance of the magnetopolaron at finite temperatures. Accordingly, our theoretical outcome may guide further experimental and theoretical investigation of the temperature characteristics of the interface magnetopolaron over the whole magnetic field region.

5. Conclusions

We have taken into account the interaction of an electron with both BO phonons and IO phonons to study the cyclotron resonance of a magnetopolaron at the interface of a polar crystal by using the Green's function method at finite temperatures. We have investigated the dependence of the cyclotron resonance mass and cyclotron resonance frequency of the interface magnetopolaron on magnetic field and temperature in the off-resonance magnetic field regions by incorporating both the absorption resonance and emission resonance. Explicit expressions have been obtained for the effective Hamiltonian of our system, and equations for calculating the cyclotron resonance mass and cyclotron resonance frequency have also been derived. Our numerical results show that the cyclotron resonance mass (cyclotron resonance frequency) is an increasing (decreasing) function of temperature when the magnetic field is lower than the resonant magnetic field, but it is a decreasing (increasing) function of the temperature when the magnetic field is higher than the resonant magnetic field. Also, the effects of IO phonons are seen to be important in determining the large-polaron characteristics near the interface. The interesting opposite temperature behaviour of the interface magnetopolaron obtained for the off-resonance regions merits future experiments to support this result.

Acknowledgment

This work was supported by the Ministry of Education of Korea through Grant No BSRI-97-2431. One of us (B-H Wei) acknowledges also partial support from GuangDong Provincial Natural Science Foundation of China.

References

[1] Devreese J T and Peeters F M 1984 *Polarons and Excitons in Polar Semiconductors and Ionic Crystals* (New York: Plenum)
[2] Larsen D M 1984 *Phys. Rev.* B **30** 4597
Larsen D M 1984 *Phys. Rev.* B **30** 4807
[3] Wu X and Peeters F M 1997 *Phys. Rev.* B **57** 9333
[4] Hai G Q, Peeters F M and Devreese J T 1993 *Phys. Rev.* B **47** 10 358
[5] Wei B H and Gu S W 1991 *Phys. Rev.* B **43** 9190
[6] Peeters F M, Wu X and Devreese J T 1986 *Phys. Rev.* B **33** 4338
Peeters F M, Wu X and Devreese J T 1986 *Phys. Rev.* B **34** 1160
[7] Yokota T 1953 *Busseiron Kenkye* **69** 137
[8] Saitoh M 1980 *J. Phys. Soc. Japan* **49** 878

[9] Arisawa K and Saitoh M 1981 *Phys. Lett.* **82A** 462
[10] Li Y C and Gu S W 1989 *J. Phys.: Condens. Matter* **1** 3201
[11] Fulton T 1956 *Phys. Rev.* **103** 1712
[12] Peeters F M and Devreese J T 1982 *Phys. Rev.* B **23** 7281
Peeters F M and Devreese J T 1982 *Phys. Rev.* B **23** 7302
Peeters F M and Devreese J T 1985 *Phys. Rev.* B **31** 5500
[13] Feynman R P 1955 *Phys. Rev.* **97** 660
[14] Osaka Y 1959 *Prog. Theor. Phys.* **22** 437
Osaka Y 1966 *J. Phys. Soc. Japan* **21** 423
[15] Wu X, Peeters F M and Devreese J T 1987 *Phys. Rev.* B **36** 9765
[16] Das Sarma S 1984 *Phys. Rev. Lett.* **52** 859
[17] Das Sarma S and Madhukar A 1980 *Phys. Rev.* B **22** 2823
Das Sarma S and Madhukar A 1983 *Phys. Rev.* B **27** 2590
[18] Wu X, Peeters F M and Devreese J T 1986 *Phys. Rev.* B **34** 8800
[19] Wei B H, Yu K W and Ou F 1994 *J. Phys.: Condens. Matter* **7** 1059
[20] Wei B H and Yu K W 1995 *J. Phys.: Condens. Matter* **8** 6695
[21] Wei B H, Zhao G Z and Gu S W 1989 *Phys. Rev.* B **40** 7866
[22] Brummell M A, Nicholas R J, Hopkins M A, Harris J J and Foxon C T 1987 *Phys. Rev. Lett.* **58** 77